# PASSIVE STANDOFF DETECTION TEAM AT SBCCOM RESULTS FROM THE OWL FIELD TEST NEVADA TEST SITE 31 JULY THROUGH 11 AUGUST 2000

James. O. Jensen[a], Agustin I. Ifarraguerri[a], Alan Samuels[a], William R. Loerop[a], Richard Matta[b], Avishai Ben-David[c],
James W. Yang[d], Christopher Gittins[e], William Marinelli[e], Thomas Gruber[f], and Dustin Grim[f]

a. Passive Standoff Detection Team, U.S. Army SBCCOM, AMSSB-RRT-DP, APG, MD 21010-5424
b. Future Sensors Branch - Aerospace C2, Intelligence, Surveillance and Reconnaissance Center, AC2ISRC/C2RI, Langley AFB, VA 23665-1993
c. Science and Technology Corp. 500 Edgewood Road, Suite 205, Edgewood, Maryland 21040
d. Geocenters Inc, Bldg E3160, rm 48, APG, MD 21010-5424
e. Physical Sciences Corp, 20 New England Business Center, Andover, MA 01810
f. Mesh Inc, 129 Bechel Road, Oxford, PA 19363

## ABSTRACT

An overview is presented of ongoing efforts in applied research by the Passive Standoff Detection Team at the U.S. Army Soldier Biological Chemical Command (SBCCOM). Passive infrared sensors such as the TurboFT, the High Sensitivity Field Fourier Transform Infrared Spectrometer (HISPEC), and the Adaptive InfraRed Imaging Spectroradiometer (AIRIS) will be described. The Owl Field Tests were held at the Nevada Test Site for a three-week period from 31 July to 18 August 2000. The AIRIS utilizes a Fabry-Perot tunable filter to spectrally resolve the image, which is captured on a 64x64-element HgCdTe focal-plane-array. The TurboFT uses a spinning crystal design to achieve scan speeds of up to 100 scans/sec with an ultimate goal of 360 scans/sec. The TurboFT utilizes a 16-element (2x8) focal-plane-array. The HISPEC is a single pixel sensor with extremely high sensitivity.

# Report Documentation Page

*Form Approved*
*OMB No. 0704-0188*



| 1. REPORT DATE | 2. REPORT TYPE | 3. DATES COVERED |
|---|---|---|
| **00 JAN 2002** | **N/A** | **-** |

4. TITLE AND SUBTITLE
**Passive Standoff Detection Team At Sbccom Results From The Owl Field Test Nevada Test Site**

5a. CONTRACT NUMBER

5b. GRANT NUMBER

5c. PROGRAM ELEMENT NUMBER

6. AUTHOR(S)

5d. PROJECT NUMBER

5e. TASK NUMBER

5f. WORK UNIT NUMBER

7. PERFORMING ORGANIZATION NAME(S) AND ADDRESS(ES)
**U.S. Army SBCCOM, AMSSB-RRT-DP, APG, MD 21010-5424; Aerospace C2, Intelligence, Surveillance and Reconnaissance Center, AC2ISRC/C2RI, Langley AFB, VA 23665-1993**

8. PERFORMING ORGANIZATION REPORT NUMBER

9. SPONSORING/MONITORING AGENCY NAME(S) AND ADDRESS(ES)

10. SPONSOR/MONITOR'S ACRONYM(S)

11. SPONSOR/MONITOR'S REPORT NUMBER(S)

12. DISTRIBUTION/AVAILABILITY STATEMENT
**Approved for public release, distribution unlimited**

13. SUPPLEMENTARY NOTES
**This article is from ADA409494 Proceedings of the 2001 ECBC Scientific Conference on Chemical and Biological Defense Research, 6-8 March , Marriott's Hunt Valley Inn, Hunt Valley, MD., The original document contains color images.**

14. ABSTRACT

15. SUBJECT TERMS

| 16. SECURITY CLASSIFICATION OF: | | | 17. LIMITATION OF ABSTRACT | 18. NUMBER OF PAGES | 19a. NAME OF RESPONSIBLE PERSON |
|---|---|---|---|---|---|
| a. REPORT | b. ABSTRACT | c. THIS PAGE | | | |
| **unclassified** | **unclassified** | **unclassified** | **UU** | **13** | |

**Standard Form 298 (Rev. 8-98)**
Prescribed by ANSI Std Z39-18

INTRODUCTION

The longwave infrared region (8 to12µm) of the EM spectrum has been used for some time at ECBC for passive detection of Chemical Warfare (CW) agents[1]. Passive LWIR detection utilizes small temperature differences between CW clouds and backgrounds for detection and alarm of a possible CW attack. This is shown in Figure (1).

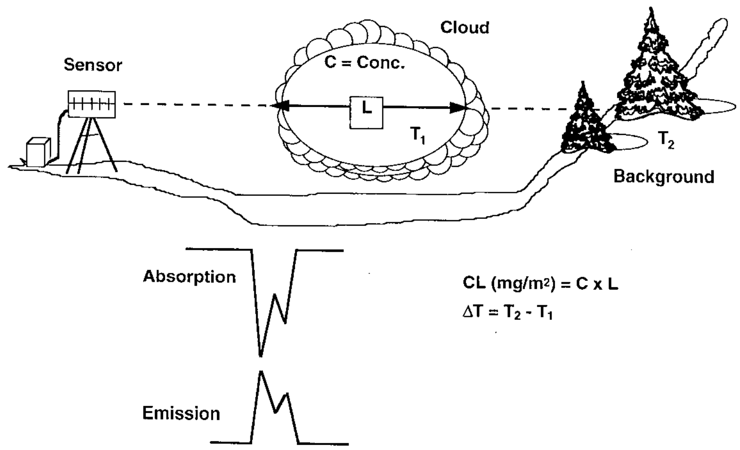


Figure 1. Principle of operation for the Chemical Imaging Sensor.

The Owl Field Tests were recently held at the Nevada Test Site. The Tests ran for three weeks from 31 July to 18 August 2000. The SBCCOM motor home spent 2 weeks in trailer park number 3, which is 1.5 kilometers form the release stacks. Three LWIR (8µm to 12 µm) passive sensors were tested. These are shown in Figure(2)

Figure 2. Three Sensors Tested – top from left to right, AIRIS, HISPEC, and TurboFT. Far right shows the three sensors as positioned next to the motorhome during the tests.

**AIRIS**– The AIRIS (Adaptive InfraRed Imaging Spectroradiometer ) is comprised of a 64 x 64 element HgCd infrared focal-plane-array (FPA) which views the farfield through a tunable piezoelectric-actuated Fabry-Perot interferometer[2] placed in the afocal region of the imaging system. The AIRIS optical configuration is depicted in figure (3).

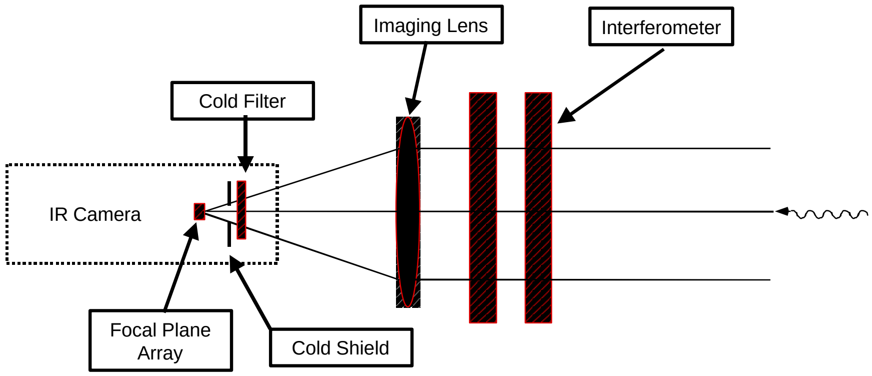


Figure 3. Diagram showing the Functioning of the AIRIS sensor.

The Fabry-Perot interferometer functions as a widely tunable, LWIR interference filter. The wavelength of light reaching the FPA is determined by the spacing of the two parallel mirrors. Light is transmitted when the mirror spacing, d, is equal to a half integer multiple of the wavelength, $\lambda$, i.e. $d = m\lambda/2$, where m is an integer. All other wavelengths are reflected. A cryogenically cooled optical filter allows only one of the transmitted wavelengths to reach the FPA.

Computer controlled selection of the transmitted wavelength takes advantage of the HgCdTe infrared focal-plane-array detector interface. The AIRIS is capable of using either sequential or selective sampling of wavelengths to build spectral data cube. Thus it is possible to tune the etalon to select wavelengths where expected chemical bands and background measurements can be made. Common pixel registry provides for simple processing for chemical cloud detection

The prototype AIRIS Spectrometer that was tested during the Owl Field Tests was manufactured by Physical Sciences Inc. The AIRIS has an operating Range from 900 $cm^{-1}$ to 1250 $cm^{-1}$. (continuous coverage of full range) with a spectral Resolution of between 8 $cm^{-1}$ and 10 $cm^{-1}$. The AIRIS has a per-pixel instantaneous field of view (IFOV) of 1.2 mrad. Noise Equivalent Spectral Radiance (NESR) of the AIRIS has been measured at $1 \times 10^{-8}$ W/($cm^2$ sr wavenumber), which is comparable to the best hyperspectral systems available in the LWIR region.

During single chemical and multi-chemical releases, the AIRIS successfully demonstrated simultaneous selective detection of individual and multiple species. AIRIS also demonstrated selective detection of single species at low column density. For example, Figure (4) represents the data taken during a DMMP release of 33 ppmv-m. At this low concentration DMMP could only be detected at a single pixel

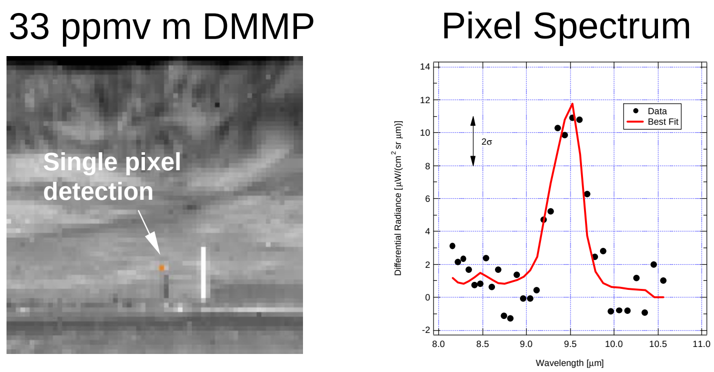


Figure 4. A 33 ppmv-m release of DMMP.   The spectrum can be extracted.

A more concentrated release is shown in Figure (5).  The plume remains hotter than background for about 10 meters.  At that point the plume cools to the temperature of the mountain in the background.  The Plume can be detected in absorption further downwind.

A Gaussian plume dispersion model was used to predict the plume temperature and DMMP concentration profile under four sets of release conditions.  The output of the plume dispersion calculation was used as input for a multi-layer atmospheric radiative transfer model to predict the wavelength dependent radiance reaching the sensor.  Figure (6) depicts the calculated differential radiance at 9.5 μm, corresponding the maximum in the DMMP emission spectrum, as a function of distance downwind of the DMMP plume release point along with the experimentally determined differential radiance.  The plume rapidly cools and dilutes resulting in a rapid decrease in peak differential radiance.  The measured plume radiance and detected plume length is consistent with local meteorological conditions (avg. wind velocity, Pasquill Class C (slightly unstable) atmosphere), plume release temperature, chemical concentration, and sensor NESR.

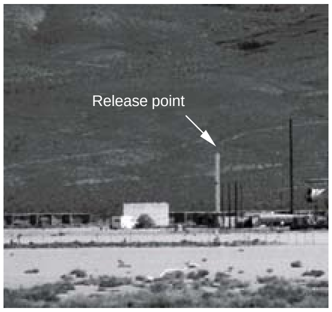


Visible image of chemical plume release stack

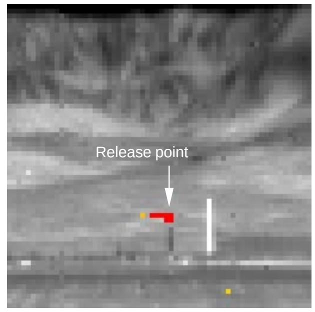


Broadband IR image w/automated plume detection

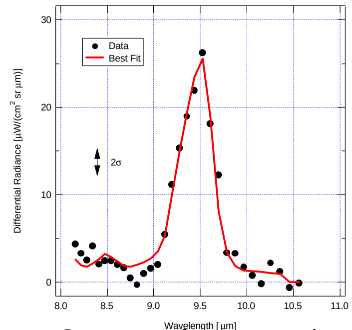


Spectrum of representative pixel w/DMMP detect

Figure 5. Release shown above is DMMP (~1800 ppmv, 160 deg C). Hot plume observed in emission (red = probable detect, yellow = possible detect) 8 frame avg., tint = 1.44 ms, 1.5 km stand-off.

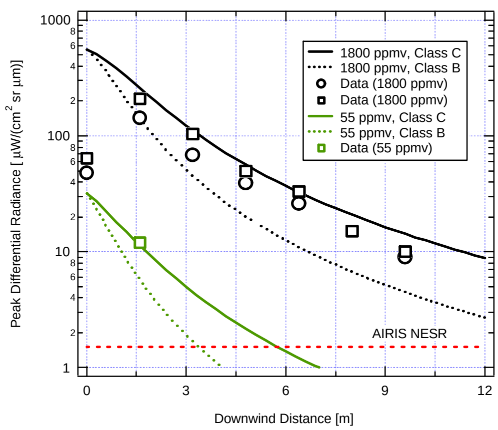


Figure 6. Four DMMP releases analyzed in detail. Meteorological station provides wind speed, direction near release point: 7 m/s avg. (12 m/s max, 3 m/s min), dir = SW. Measured plume radiance and detected plume length consistent with local meteorological conditions (avg. wind velocity, Pasquill Class C (slightly unstable) atmosphere), plume release temperature, chemical concentration, and sensor NESR.

**TurboFT** - The Chemical Imaging Sensor (CIS) is currently a sixteen-pixel system utilizing the TurboFT Spectrometer developed by Designs and Prototypes.[3] The major benefits of the TurboFT over other conventional Fourier Transform Spectrometer (FTS) designs is the extremely high-speed operation (hundreds of scans per second), the ability to run without a laser, and the very small size and low weight. The high speed is the direct result of the rotary scan technique using a mass balanced rotor design. A comparison of the TurboFT design and a conventional Michelson FTS is shown in Figure (7). Since there is no scan direction reversal (a characteristic of the Michelson interferometer) in the TurboFT, the operation is very smooth and stable. Most vibrational disturbances, which would otherwise affect spectral quality, are eliminated. Speed of operation is limited more by constraints in signal electronics than by mechanical parameters. The laser-less operation is also a direct benefit of the rotary scan.

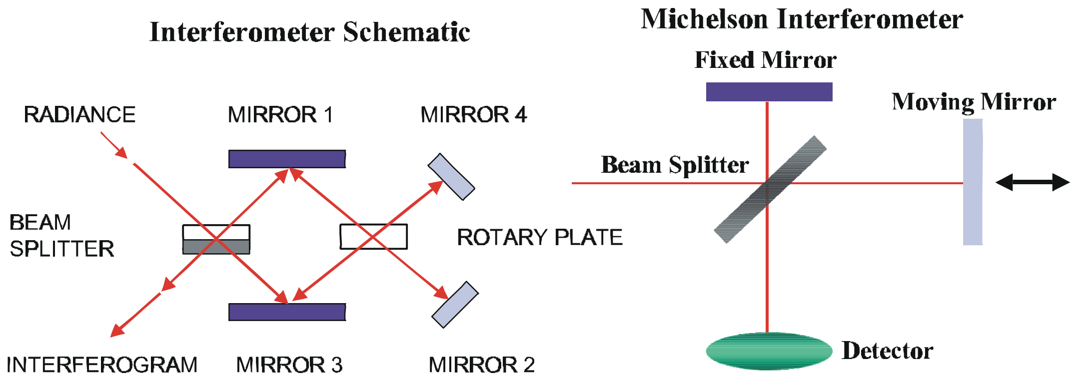


Figure 7. Comparison of the TurboFT interferometer vs. a traditional Michelson design. The TuboFT is very simple in its design. It has no laser and is very small and lightweight. It also is capable of operating at very high speeds.

The sixteen-element focal-plane array is shown schematically in figure 8 with its current pixel arrangement of 2 x 8. Each pixel represented a rectangle of approximately 2 meters by 10 meters when sensing from a distance of 1.5 Kilometers.

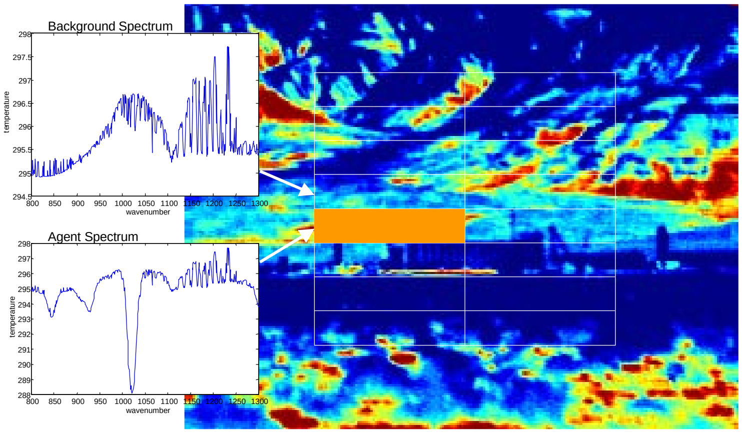


Figure 8. The current arrangement of the sixteen-element focal-plane array in the TurboFT. The current system is bore sighted with a visible camera. At a distance of 1.5 kilometers, each pixel covers an area of approximately 2 meters by 10 meters.

At the Owl Field Tests the TurboFT operated at very high speeds approaching 100 scans/sec with good results. Figure (9) represents the special ratio of some data taken on 4 August 2000. The Special Ratio is defined to be:

$$SR = \frac{release - blackbody}{background - blackbody}$$

As seen in Figure (9), the peak near 950 $cm^{-1}$ can be attributed to the $SF_6$ in the release.

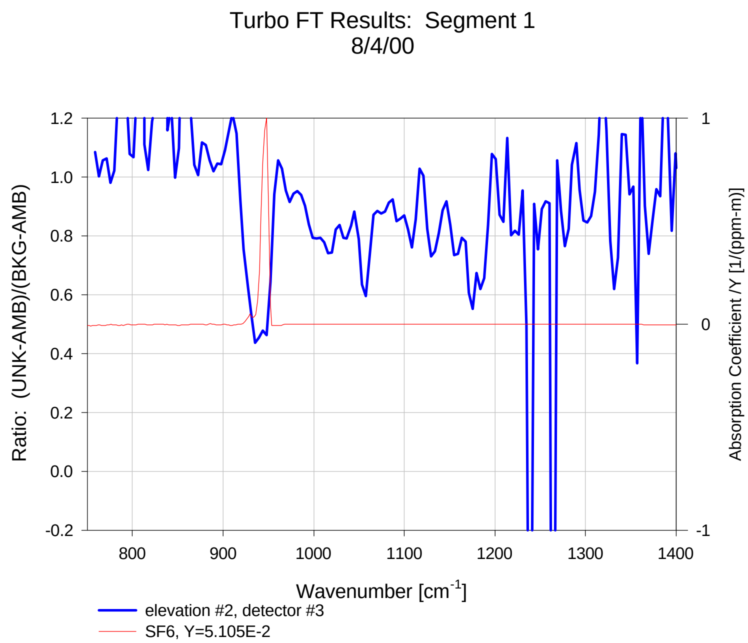


Figure 9. Special Ratio of data taken of an $SF_6$ release using the TurboFT at the OWL Field Tests.

Since the Chemical Imaging Sensor will be required to operate “on the move”, we have been working on algorithms that do not require background subtraction. In Figure 10 we show the same data sets analyzed using the Mesh Algorithm.

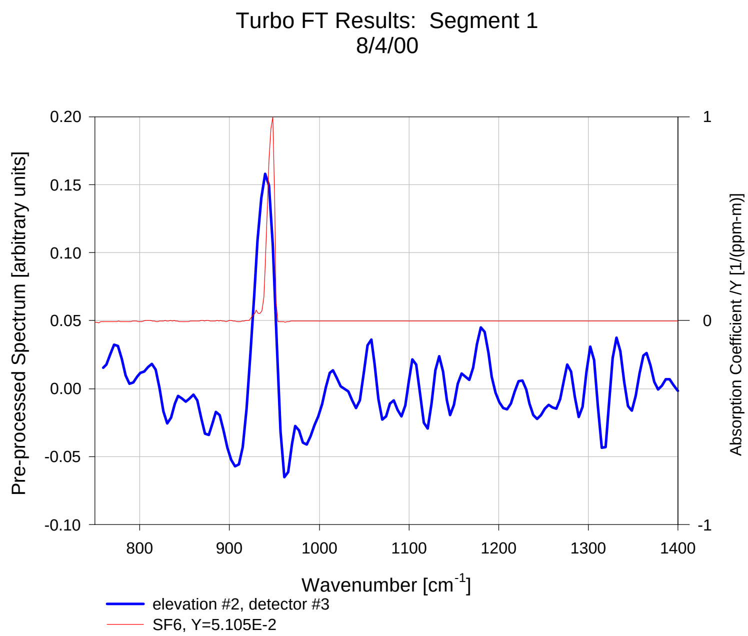


Figure 10. Analysis of data taken of an SF6 release using the TurboFT at the OWL Field Tests using the Mesh Algorithm.

**HISPEC** – The HISPEC (High Sensitivity Field Fourier Transform Infrared (FTIR) Spectrometer) is a traditional Michelson single-pixel field spectrometer. However the HISPEC was designed to be ultra-sensitive with an extremely low single scan NESR[4] ($2 \times 10^{-10}$ watts/(cm$^2$ sr wavenumber) ). The HISPEC, manufactured by Block Engineering, is probably the most sensitive FTIR spectrometer in the world. This high sensitivity was achieved with several innovations. Notable among the unique properties of the HISPEC are the ultra-stable reference channel and its signal channel electronics.

The requirement of increased system sensitivity places an increased burden on the detector parameters and the signal channel electronics. Throughout the design of the signal channel, great care has been taken toward minimizing sources of performance-limiting noise and preservation of a large dynamic range. Since the HISPEC is envisioned for possible mass production at some time in the future, hand selection of components was avoided. Design parameters dictated that sensitivity improvements must be the result of improvements in the core design combined with better matching of the final sensor to a given application.

The primary factors involved in the sensitivity improvement are increased throughput (increased target photon collection), a detector carefully matched to the collection optics (throughput matching), increased dynamic range, and higher sampling stability. The detector must also be matched with the signal channel electronics to take full advantage of the greater signal levels. This demands optimal detector cold shielding, a detector-noise-limited/wide dynamic range preamplifier, a post-amplifier with the correct bandwidth filtering and the equivalent of true 20+ bit analog-to-digital (A/D) converter performance.

In order to achieve maximum sensitivity, a properly designed signal channel must preserve the detector noise from the analog input throughout the digitization process (i.e. the noise introduced during the digitization process must not be significant relative to the detector noise). This means that the analog noise must be equal to or greater than the least significant bit in the A/D converter. If this condition is not met, then the A/D board is throwing away information and thus sensitivity. Modeling has shown that a standard 16-bit A/D board, commonly present in interferometers manufactured today, is not sufficient. In order to be "detector noise-limited" the dynamic range of the instrument must be increased.

The current HISPEC uses a gain-ranging technique to obtain an effective 22 bits of resolution. Thus, the centerburst of the interferogram is digitally captured while at the same time preserving resolution at the wings of the interferogram. This is shown in figure(11). This is accomplished by running two simultaneous analog post-preamplifier signal chains whose gains are set by a factor of sixteen (4 bits) apart. The system utilizes a single wide dynamic range preamplifier, which feeds the two different post amplifiers simultaneously. At the beginning of each scan, the analog multiplexer (MUX) connects the output of the low-gain post-amplifier to the A/D. At a selected point in the interferogram, the MUX switches to the high-gain post-amplifier and then presents the signal to the 18-bit A/D converter for conversion (after passing through an electronically programmable low-pass filter). The purpose of the programmable filter is to allow operation at more than one pre-selected retardation (spectral output) rate with the change in band of inteferometer frequencies that occurs. We have at the output of the A/D 18-bit words, which correspond to the 1X output up to the point where the counter/latch switches the MUX to the 16X gain output. At the corresponding time, the amplitude of the digital words taken at the higher gain is divided by 16. This is done by shifting the words 4 bits toward the least significant bit. In this way the interferogram is fully corrected and the change in gain is transparent to the computer and the user. Since the change in gain is done by multiplexing, no spurious signals are generated.

The high sampling stability of the interferometer is achieved by placing the optical reference signals (white light and HeNe laser) in the center of the optical axis, thus making them immune to mirror tilt. The result is significantly improved sampling and phase stability, which translates into higher sensitivity

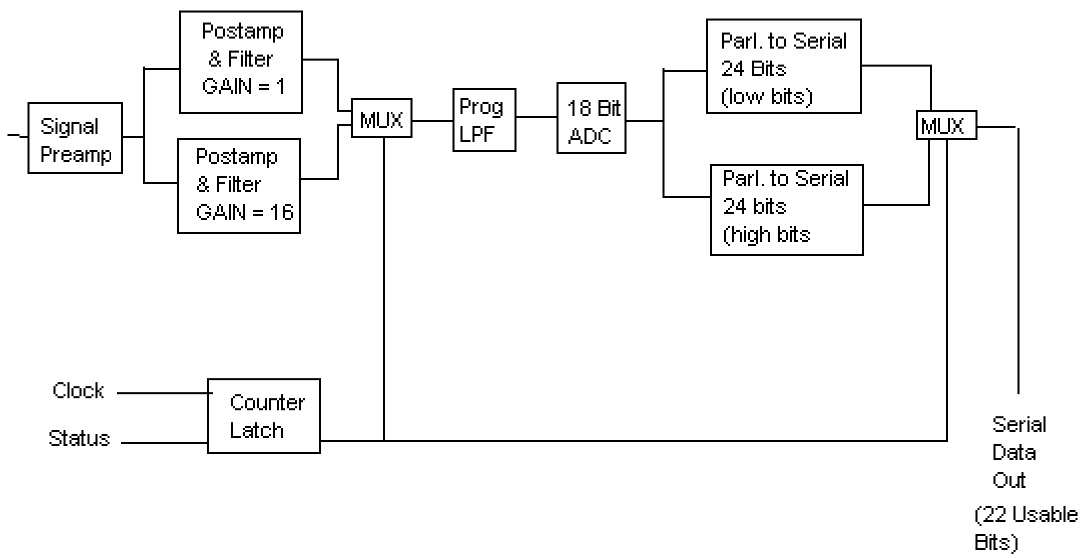


Figure 11. Digitizing Electronics in the HISPEC.

At the Owl Field Tests the pixel size of the HISPEC was approximately 10 meters square. While this does not match the stack size exactly, it gave some very good data. The detection of individual chemical species was performed using a matched filter technique. This is shown in Figure (12). After converting the radiance spectra to pseudo-transmission (i.e. un-scaled transmission), the influence of the atmospheric absorption was suppressed using the orthogonal projection operator:

$$\mathbf{P} = \mathbf{I} - \mathbf{U}\mathbf{U}^T$$

where **U** is the orthonormal matrix containing the first few principal vectors of the matrix formed by all the pseudo-transmission spectra for a given day of collection. Typically, **U** consists of either one or two column vectors, since the atmospheric transmission is the primary contributor to the spectra. The matched filter score is then obtained by:

$$score = \frac{\mathbf{x}^T \mathbf{P}\mathbf{t}}{\mathbf{t}^T \mathbf{P}\mathbf{t}}$$

where **x** is the column vector containing the pseudo-transmission and t is the target column vector obtained from a spectral library. A score of 1.0 or -1.0 represents an exact match (the sign indicates emission or absorption).

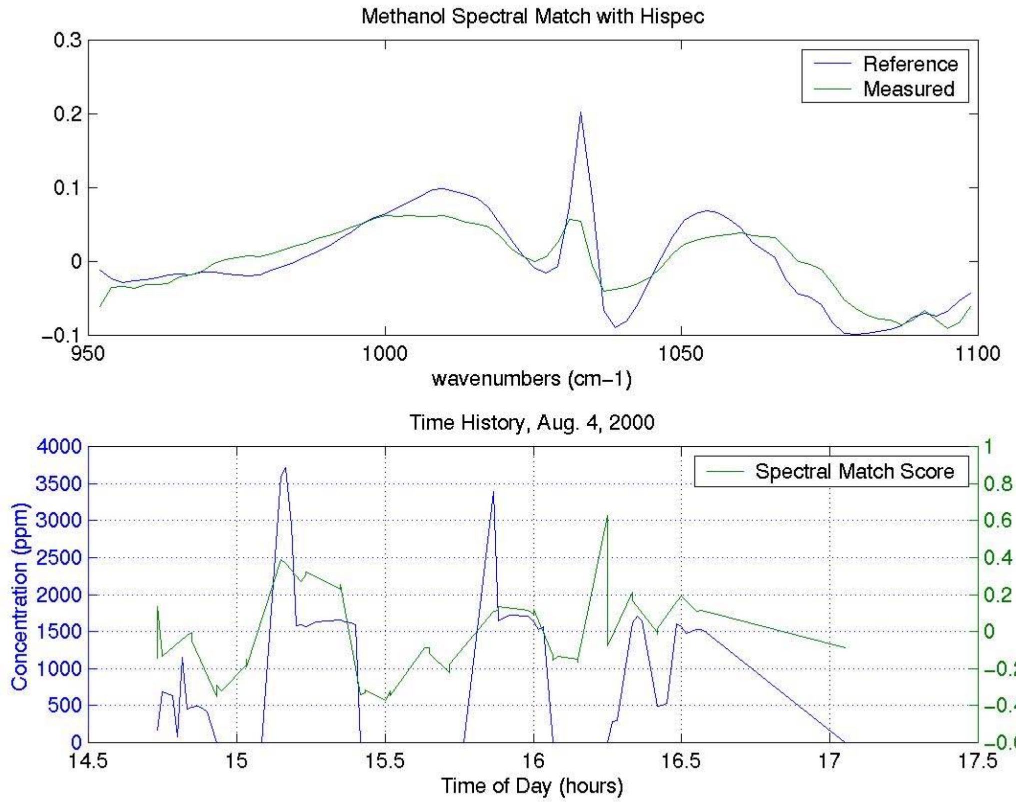


Figure 12. Top spectrum of methanol extracted from the HISPEC data. Below is the spectral match score, which gives an estimate of the concentration of methanol from the stacks.

## SUMMARY AND CONCLUSION

The goal of the JSWAD program is to produce imaging spectrometers that maintain high chemical detection sensitivity while operating at very high acquisition rates. Detection "on-the-move" scenarios are very important to many DOD Joint Service applications, as is the ability to "look" everywhere at once without scanning. High sensitivity must be maintained in order to sense chemicals as relatively low concentrations a distances of up to several kilometers. Three sensors were recently tested at the Owl Field Tests at the Nevada Test Site in support of the Joint Service Wide Area Detection (JSWAD) Program. The TurboFT, AIRIS, and HISPEC spectrometers were evaluated with good success.

## REFERENCES


1. W.R. Loerop, "Feasibility Of Detecting Chemical Agents Using a Chemical Imaging Interferometer From Low and High Altitude Platforms". U.S. Army Edgewood Research Development and Engineering Technical Report, ERDEC-TR-381, (1996)

2. C.M. Gittins, W.G. Lawrence, and W.J. Marinelli, "Frequency Agile Bandpass Filter for Direct Detection Lidar Receivers," Appl. Opt. **37**, 8327-8335 (1998); W.J. Marinelli, C.M. Gittins, A.H. Gelb, and B.D. Green, "Tunable Fabry-Perot Etalon-Based Long-Wavelength Infrared Imaging Spectroradiometer," Appl. Opt. **38**, 2594-2604 (1999)

3. W. Wadsworth and J.P. Dybwad, "Ultra High Speed Chemical Imaging Spectrometer", Proc. Of Electro-Optical Technology for Remote Chemical Detection and Identification II, Vol 3082, pp 148, SPIE, Bellingham, WA (1997); W. Wadsworth and J.P. Dybwad, "Chemical Imaging Spectrometer", Proceedings of the Fourth Joint Workshop on Standoff Detection, Williamsburg, VA, Science and Technology Corp., Oct. 1998.

4. T.G. Quinn, R.F. Conners, C. Fehser, J.A. Flanagan, D.E. Grover, E.R. Schildkraut, J.O. Jensen, and W.R. Loerop, "Optimized, High Sensitivity, Field FTIR Spectrometer – HISPEC", Proceedings of the Fourth Joint Workshop on Standoff Detection, Williamsburg, VA, Science and Technology Corp., Oct. 1998.